

EXECUTIVE SUMMARY

LTX- β has successfully (but belatedly) completed the scope of the first FES Notable Outcome for FY2021, which was due on March 31, 2021. The FES Notable Outcome is restated here:

On the LTX- β experiment, extend Ohmic plasma current operation with fully coated solid and liquid lithium walls to greater than 0.125 MA. Using kinetic equilibria, estimate the energy confinement time of low-recycling LTX- β plasmas, which connects to previous LTX Ohmic results, and submit a report documenting the findings to DOE by March 31, 2021.

LTX- β has now been operated at plasma currents of up to 0.137 MA, with diagnostics including Thomson scattering and ion temperature measurements from spectroscopy. Operations with liquid lithium walls at 200°C achieved 0.129 MA. This is a marked increase in plasma current from results reported for the January 2020 Notable Outcome, which were limited to ~ 0.075 MA for cold walls, with hot wall operations limited to <0.060 MA. Electron temperatures in the 300 – 400 eV range have been produced, for both cold and hot shell operation. These electron temperatures are the highest yet recorded for LTX- β . Flat electron temperature radial profiles have also been documented, which persist for several confinement times – another first. Measured ion temperatures from C VI emission are ~ 150 eV. Data from these temperature measurements has been used to constrain kinetic equilibrium reconstructions with both solid and liquid lithium wall coatings, and produce estimates of the energy confinement time during ohmic operation. The submission of this report thus fulfills the requirements of the DOE notable outcome cited above, although we were unable to produce these results by the due date of March 31, due principally to delays caused by the global pandemic, infrastructure deficiencies, and toroidal field coil arcing issues.

INTRODUCTION

The major research goal for the LTX- β group in FY2021 is to continue to document plasma energy confinement as the global recycling is varied over a wide range through the use of lithium plasma-facing surfaces. In order to adequately document energy confinement in a low aspect ratio tokamak, equilibrium reconstructions which are constrained by Thomson scattering temperature and density profiles are required. Measurements of the core ion temperature with charge-exchange recombination spectroscopy (CHERS) are another constraint applied to reconstructions.

FACILITY IMPROVEMENTS

In late FY15 two neutral beam systems were obtained as a no-cost loan from Tri-Alpha Energy. The beam source installed on LTX- β has produced >700 kW of auxiliary heating, with >35 A of core fueling. The source has been operated very successfully over an accelerating voltage range of 16 – 23 kV, which exceeds the original specifications of the Budker system, due to improvements made at PPPL. Recently, over 800 kW has been extracted from the neutral beam (Figure 1).

Corrections to the CHERS data analysis permit ion temperature and toroidal rotation measurements at the lowest injection energy, although this is near the minimum energy which has ever been employed for CHERS. The beam as originally provided could not be operated reproducibly due to shot to shot variations in the gas supply. During the first quarter of FY20 the original gas valves and drivers were replaced with precision fast valves from Parker Hannefin and PPPL-designed valve drivers, which are much more reproducible, and do not require frequent service. The power supplies provided with the beam have been found to require significant maintenance and support.

A previously unused field coil power supply, manufactured by P=EI, and originally in use on the PBX-M tokamak until the early 1990s, has been completely rebuilt, and now operates in series with one of the Robicon-manufactured LTX field coil power supplies, to increase the voltage supplied to the toroidal field coil to 800V, at 5,000A. The new power supply set has increased the operating toroidal field to approximately 3.2 kG.

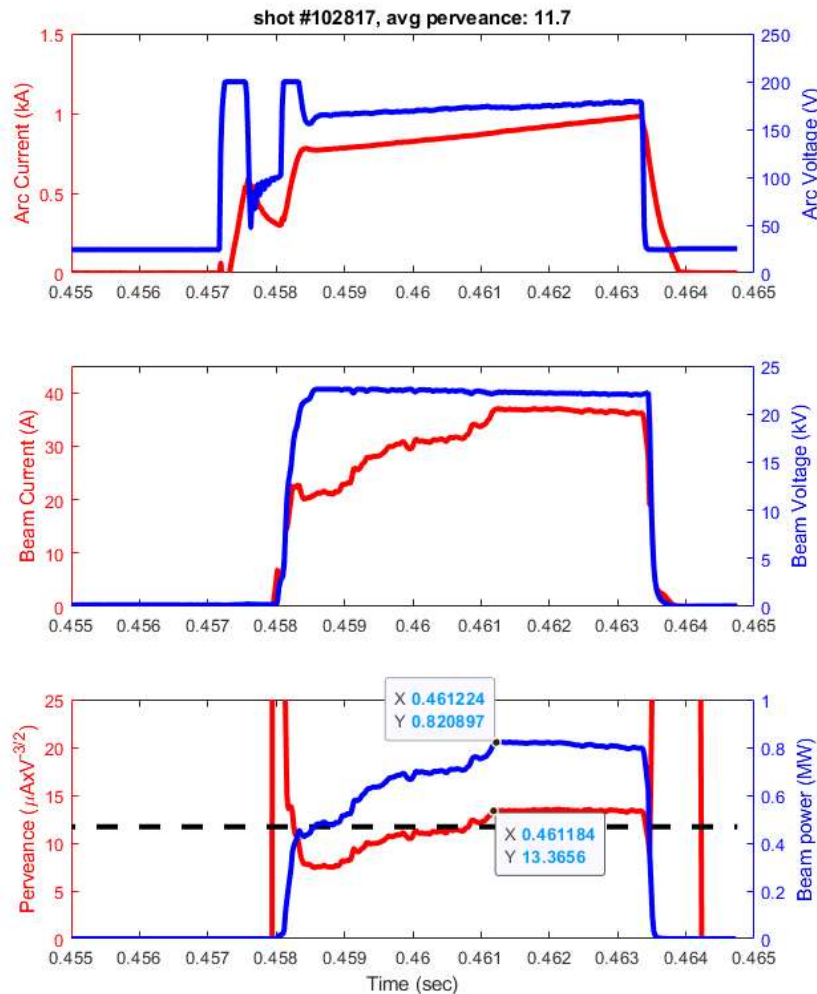
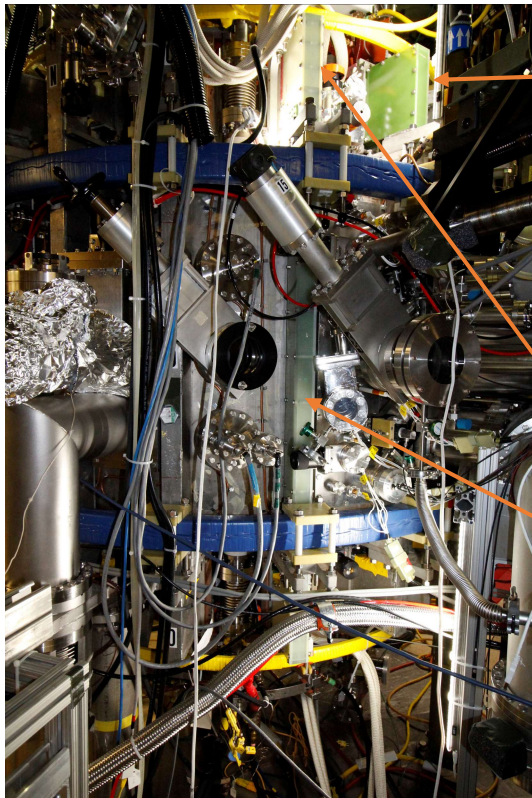


Figure 1. The TAE neutral beam has now been operated at 23 kV, with a peak extracted power of 800 kW. However, the beam perveance is lower than in operation at 16 kV, and fast ion confinement is improved at the lower operating voltage. Hence beam operations in 2021 will focus on lower (16 kV) operating voltage.

Operation at higher field has increased the maintenance requirements for the LTX-β toroidal field coil set – the centerstack dates to 1994, and the outer TF legs to the 1980s, with a design field of 0.9 kG. In two separate instances, arcing to the grounded aluminum case used on the TF coils has interrupted operations and required repair. In the first case, which occurred at the start of FY21, it was necessary to partially replace the case of one TF coil, as well as a section of OH bus which was involved in the arc. This repair took approximately five weeks to complete. A second arc in March 2021, caused by a small water leak into the original, partly open aluminum case, required a full removal of the entire aluminum case. The TF conductor insulation was completely removed and replaced with multiple layers of Kapton insulation, while a new G10 (fiberglass) case was constructed and installed. This task was accomplished in situ, without breaking vacuum or any disassembly of the poloidal field coil set, in six weeks, beginning March 18, 2021. Figure 2 is a photograph of the fully rebuilt TF coil, and its partially rebuilt neighbor.

Prior to FY21, the plasma current was limited to approximately 100 kA, using one half of the full ohmic power supply. The second half of the ohmic power supply has now been brought online and integrated with the original half supply. The Ohmic power supply now consists of two 0.4 MJ capacitor banks, each of which powers a full H-bridge with 28 IGBTs. The two H-bridges are connected in parallel to power the ohmic solenoid. This arrangement doubles the current capability of the ohmic power supply, and increases the available pulse length. A photograph of the recently completed power supply is shown in Figure 3.



Partially recased coil

Figure 2. Photograph of the fully and partially re-cased TF coils

Fully recased coil



Figure 3. Photo of the full ohmic power supply. The original capacitor bank is to the left, the new bank is to the right. The IGBT-based H-bridges and the buswork are at the far end of the capacitor banks.

In Figure 4 we show plasma current traces, obtained with the upgraded power supply, and compared to the previous highest plasma currents obtained, for both cold and hot shell operation, in LTX- β . With the new power supply it has so far proven possible to increase the current in cold shell discharges by

approximately 40%, and to approximately double the maximum current in hot wall discharges. The new power supply has only been operated at 80% of the expected maximum in stored energy, to date.

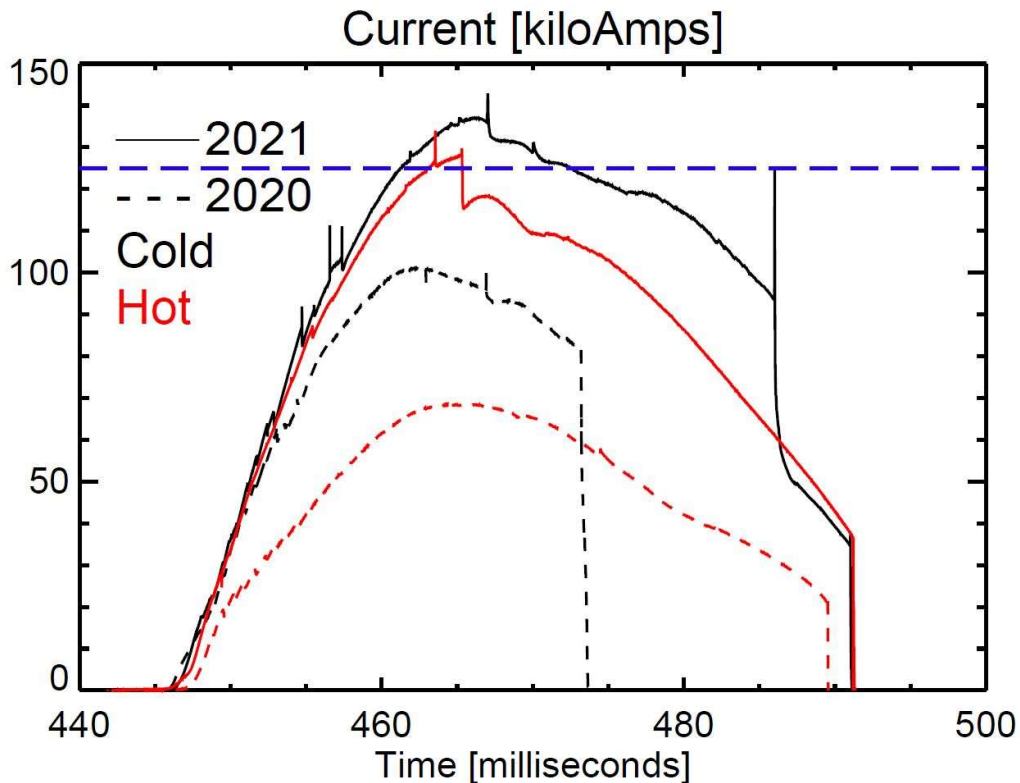


Figure 4. Plasma current for discharges with the upgraded ohmic power supply (solid traces), with both cold (solid lithium coated) and hot (liquid lithium coated) shells. The dashed blue horizontal line indicates the 125 kA target. Also shown are the highest current discharges (dashed traces) obtained with hot and cold shells, prior to the power supply upgrade, for comparison. MHD activity is responsible for the sharp drop in current in both discharges at ~ 465 msec.

A CHERS diagnostic has been added for ion temperature and toroidal rotation measurements (ORNL task, with participation from PPPL). The diagnostic has been operational since early CY20, and has yielded past measurements of the core ion temperature, to constrain equilibrium reconstructions. For the data presented here, which focuses on ohmic plasma operation, ion temperatures are provided by measurements of the Doppler broadened width of the 529 nm C VI line. The UCLA profile reflectometer has been upgraded to provide measurements of core density fluctuations. Final installation of the new system is now underway. A suite of scrape-off layer (SOL) diagnostics, including Langmuir probes, in addition to edge spectroscopy have been installed to document the collisionless SOL expected in LTX- β . A previous installation of low field side Langmuir probes suffered from slideaway electron damage; the new LFS Langmuir probe has been moved off the machine midplane. A sample exposure probe, operated in collaboration with ORNL and Princeton University, will document the condition of the lithium wall coatings. In addition, the Princeton University surface group will deploy a new approach to the measurement of SOL layer ion energy and impact angle, which employs micro-trench samples. This approach has been previously deployed on DIII-D by Shota Abe, who is also performing the work on

LTX- β . Other improvements to the diagnostic set include additional spectroscopy, upgrades to the magnetic Mirnov coil and flux loop sets, and lithium deposition monitors. The system of viewing optics for the Thomson scattering system is being expanded to include five additional sightlines on the plasma axis, and to the high field side of the axis, in order to increase the fidelity of electron temperature and density profiles, and further constrain equilibrium reconstructions and energy confinement estimates. The original Thomson system cannot view to the high field side of the plasma axis due to reflections from the lithium-coated shells, which produce excessive stray light. In order to produce Thomson-constrained equilibria and confinement estimates between-shots, the HFS system will employ the detector and data acquisition system originally procured for the SOL Thomson system, rather than another Princeton Instruments camera-based detector, which is partly responsible for low signal levels in the existing core system. The General Atomics-designed polychromator system has significantly greater light gathering capability and throughput than the camera-based core detector system.

The supersonic gas injector (SGI) which was developed on CDX-U, duplicated for NSTX, and had been installed on LTX, has now been refurbished and modified (heat shielded, gas cooled, and temperature-instrumented) for use during hot shell operation in LTX- β . The SGI is bellows-mounted, and will be used to fuel the plasma while inserted into the upper SOL through an access duct in the shells, at a major radius of $R=45$ cm. The SGI produces short gas pulses with high fueling efficiency, without the long decay time of gas puffs supplied by the centerstack gas nozzle. We will use the SGI for density sustainment with minimal neutral gas influx to the SOL, and for particle confinement time studies.

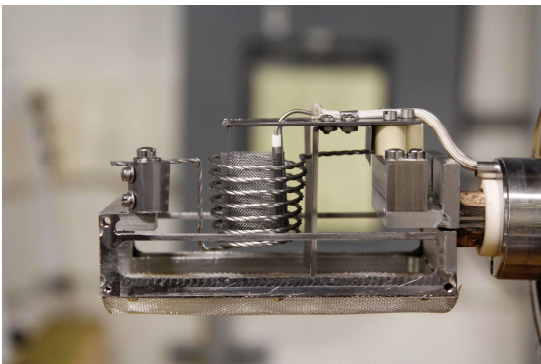


Figure 5. Redesigned lithium evaporator.

The lithium evaporator system has been redesigned, for both easier refilling and for a $20\times$ increase in the lithium inventory. In the first test of the new evaporator, 5 grams of lithium was loaded into each of the two evaporators; the previous evaporator design had a maximum capacity of 0.5 grams. The new evaporator (shown in Figure 5) can also be scaled for use in other tokamaks, such as NSTX-U, or ST40, which is operated by Tokamak Energy in the U.K. For the results reported here, we typically evaporated a coating approximately 100 nm thick of lithium onto the shells just prior to commencing tokamak operations.

RESULTS

Scrape-off layer temperature

In 2019 a movable low field side Langmuir probe was installed at the outer midplane of LTX- β . The probe yielded initial data on scrape-off layer (SOL) density and temperature, but was badly damaged during operations. In 2020, a new more robust probe was constructed, and installed in an off-midplane port, to avoid damage by slide-away electrons occasionally produced during low density operation with lithium coated walls. The new probe has demonstrated the differences in the SOL with passivated lithium

walls, versus fresh solid and liquid lithium coated walls. The probe results also highlight the need for SOL Thomson scattering.

Operation with passivated lithium walls yields the coldest and densest SOL plasma. This data was taken approximately a year after the last lithium coating was applied to the shells (LTX- β has now been under vacuum since summer 2018). In Figure 6 (a, b, and c) the Langmuir probe density and temperature measurements are shown, along with the line density from the interferometer. Note that in the case of passivated lithium walls, the maximum plasma current was < 50 kA, and the probe was 2 cm inboard of the shell radius (or $R=64$ cm, mapped to the midplane). Plasma temperatures in the SOL were ~ 25 eV (Figure 6a). Operation with either hot or cold, freshly lithium-coated walls, yields SOL plasmas with electron temperatures approaching 100 eV (Figures 6 b&c). The temperature measurements shown in Figure 6 (b&c) were taken with the Langmuir probe tip flush with the surface of the lithium-coated shells. An electron temperature of 100 eV *up to the wall* strongly supports the expectation that, with lithium walls, plasma electrons will impact the walls at full energy – there is no cooling mechanism for the SOL plasma; the particles retain full energy as they enter the wall, and slow down via elastic scattering in the layer of lithium on the wall. 50 - 100 eV electron temperatures are also excessive for measurement with a Langmuir probe, and underscores the need for edge Thomson scattering in LTX- β .

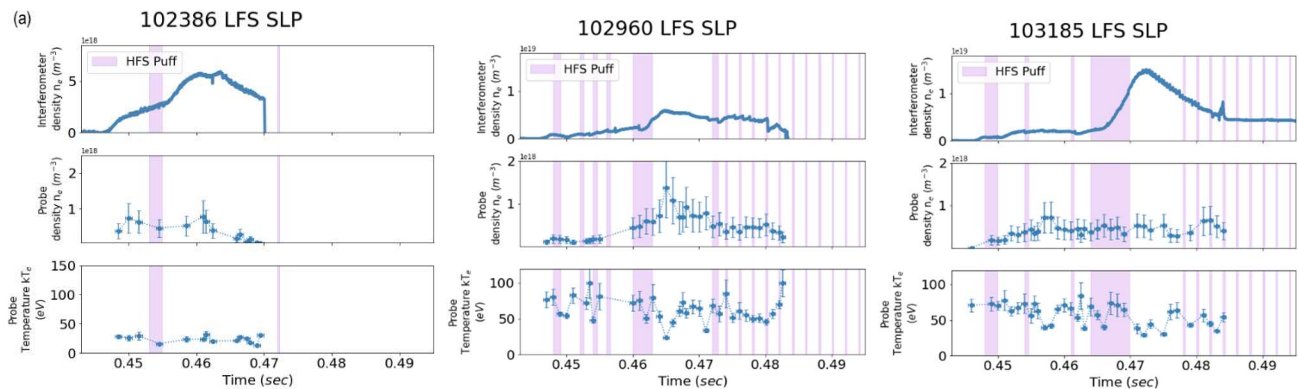


Figure 6 (a, b & c). Low field side scrape-off layer swept Langmuir probe (SLP) measurements with (a) passivated lithium walls, (b) recently coated cold (solid) lithium walls, with peak plasma current = 130 kA, and (c) recently coated hot (liquid, 200 °C) lithium walls, with peak plasma current = 127 kA. Note that the pink shaded areas denote the time and duration of centerstack gas puffing.

Earlier results from LTX with flat temperature profiles highlighted the low collisionality of the scrape-off layer (SOL). These most recent results indicate similar low edge collisionality. In Figures 7 and 8 are shown contour plots of \mathbf{v}_e^* and \mathbf{v}_i^* for both cold and hot shell operation. The discharges with solid lithium (cold shells), corresponding to Figure 6(b), employed less gas puffing, with a gas puff which ended at $t \sim 0.462$ sec, and no fueling at all within the time window shown in the contour plots of collisionality. In contrast, the discharges with liquid lithium walls (hot shells) employed a large gas puff within the time window for the contour plot of collisionality. A low collisionality boundary is quickly recovered.

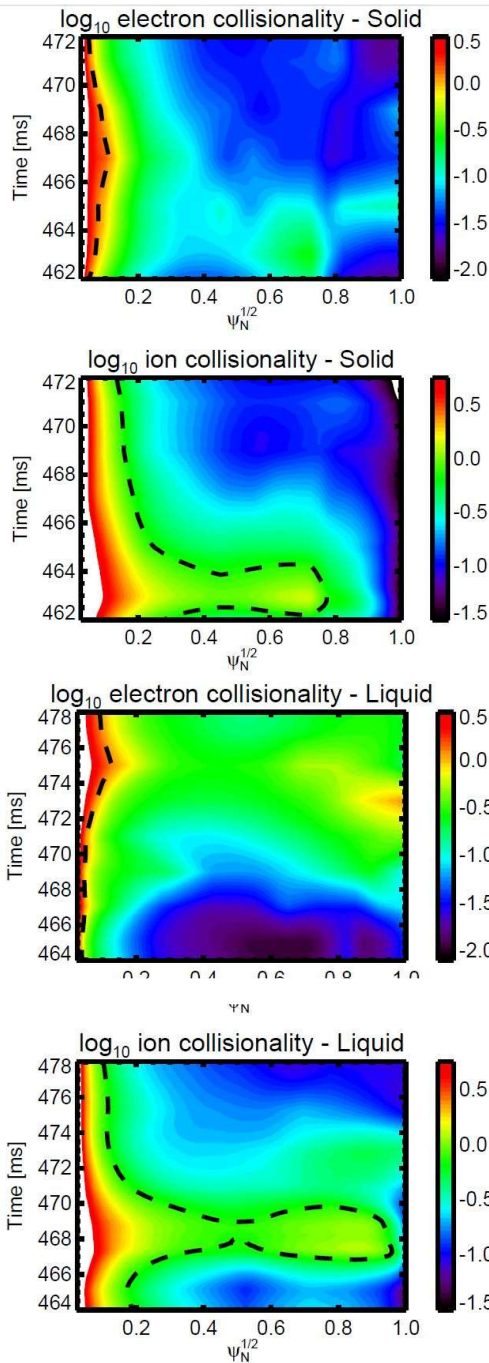


Figure 7. Contour plots of electron and ion collisionality (from TRANSP) for discharges with solid lithium walls. The time window is restricted to the available Thomson scattering and ion temperature data. The dashed lines in the plots denote the boundary of the banana regime.

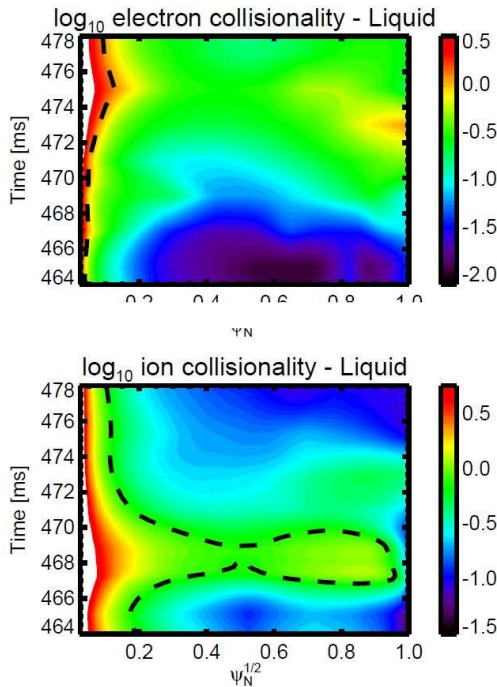


Figure 8. Contour plots of electron and ion collisionality (from TRANSP) for discharges with liquid lithium walls (hot shells at 200 °C). The time window is again restricted to the available Thomson scattering and ion temperature data.

Trapped particle effects are expected to introduce important modifications to the SOL and power flow to the high field side limiting surface in this case. We are working to reconcile the kinetic LTX-β SOL with the fluid SOL assumed in DEGAS2.

Core electron temperature

Electron temperature profiles have been determined via Thomson scattering for discharges with cold shells (solid lithium coated) and hot (200 °C), liquid lithium coated shells, with peak plasma currents of 125 – 130 kA. A summary plot of the results is shown in Figures 9 (for cold shells), and 10 (for hot shells). Since the Thomson scattering system laser system only provides a single laser pulse per

discharge, a determination of the evolution of the electron temperature requires several discharges, while the laser firing time is stepped through the discharge. In addition, data from several discharges was averaged to produce the profiles.

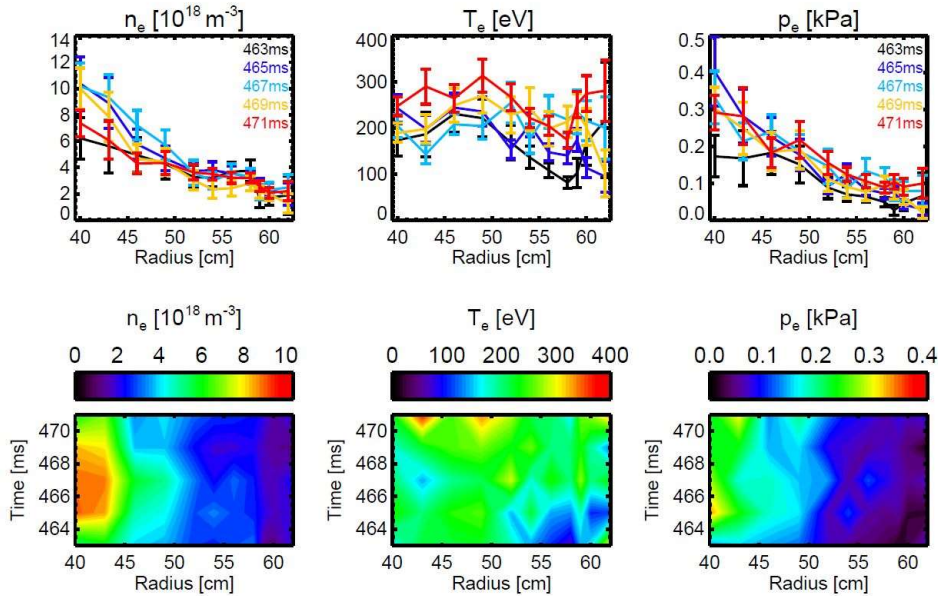


Figure 9. Electron density and temperature profiles with cold shells, near room temperature (20 °C). Electron temperature radial profiles for cold shell operation became flat as the discharge progresses. The flattening of the electron temperature is similar to the flattening seen in LTX in 2015. However, the flattening of the electron temperature profile last for much longer than in LTX.

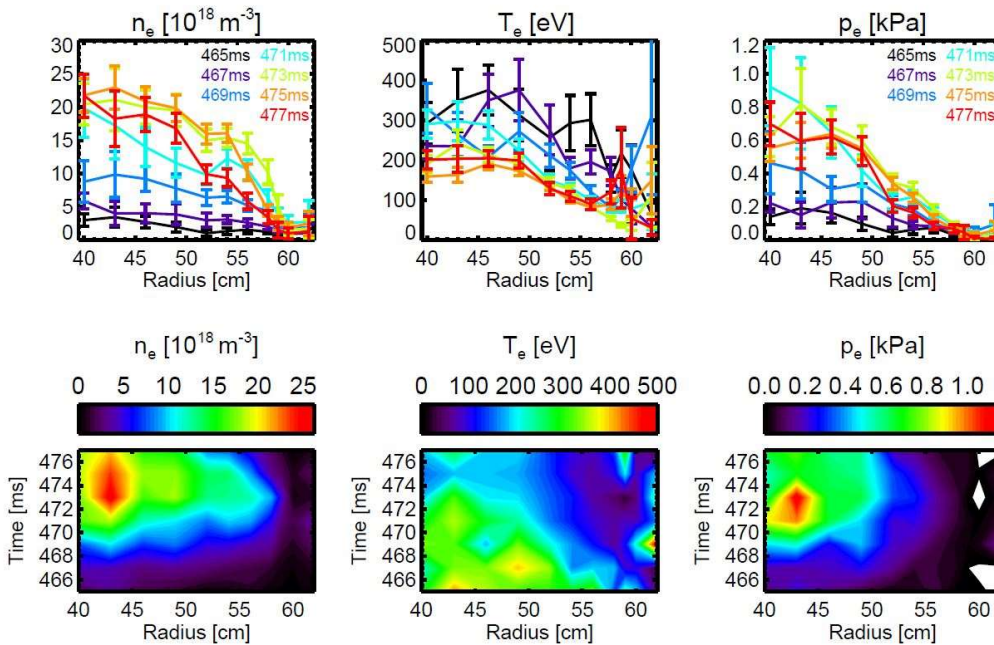


Figure 10. Electron density and temperature profiles with hot shells (200 °C). Gas fueling was higher for hot shell discharges, which raised the central electron pressure to ~ 1 kPa – roughly four times higher than was achieved during the campaign to complete the January FY20 Notable. Peak electron temperature was in the 300 – 400 eV range for both cold and hot shells. These electron temperatures are the highest yet recorded in LTX- β .

With cold shells (solid lithium) the electron temperatures were in the 200 – 300 eV range, and the radial profiles of temperature were flat. This is comparable to the highest temperatures reported for the flat temperature experiment on LTX of 250 eV (D. P. Boyle et al., Phys. Rev. Lett. 119 (2017) 015001). However, the duration for which flat temperatures persisted here was approximately 5 msec – throughout most of the available Thomson scattering data. This is several confinement times for this discharge. The original LTX experiment documented flat temperature profiles for ~ 1 msec.

Electron temperatures of up to 400 eV with liquid lithium walls are the highest ever observed on LTX or LTX- β , with solid or liquid walls, and with peak densities in range of $2\text{-}3 \times 10^{19} \text{ m}^{-3}$. A longer, broader-coverage lithium evaporation was also executed prior to the experimental campaign which produced the liquid lithium wall data. The additional lithium deposition was coincident with a noticeable day over day increase in the plasma current, of approximately 10 kA. This observation highlights the need to move to a lithium deposition system capable of between-shots operation.

Note that the present Thomson system is not capable of viewing scattered light at $R < 40$ cm, while the plasma axis in many discharges is inboard of 40 cm. This highlights the need for the high field side Thomson system, which is being installed this fiscal year.

A significant difference in the cold and hot shell discharges shown here is that the hot shell discharges required significantly more fueling to improve stability during the current ramp, resulting in higher core density and lower edge temperature. In the case of hot shells, Thomson scattering data was not available for a sufficiently long period after gas puffing was terminated to permit the edge electron temperature to rebound. The electron temperature profile remained peaked on-axis. In contrast, for the discharges with cold shells, lower gas fueling rates allowed the edge temperature to recover to the core value. The radial electron temperature profiles for the cold shell case are flat, as is expected for very low recycling walls (first demonstrated on LTX). High plasma current ramp rates, at or slightly in excess of 10 MA/sec., were employed in these discharges; in future experiments we will investigate lower current ramp rates to help avoid the internal reconnection events visible on the current traces in Figure 4 – especially for the hot shell discharges.

Core ion temperature

CHERS in LTX- β uses Li III light produced by charge exchange between the neutral beam and fully ionized Li^{3+} . The level of CX emission is much smaller than the intrinsic Li III light, and requires very careful background subtraction, using two sets of optical fibers – one which views the neutral beam, and one which only views the background plasma, through a set of four different windows (two viewing the beam, and two not). During this campaign lithium coatings on the CHERS windows or other changes from the original calibration have introduced uncertainties which have not yet been resolved. In addition, since active CHERS requires beam injection of at least 2 msec duration for a measurement, some beam heating of the ions was possible. For these discharges, estimates of the core ion temperature were instead made by measuring the Doppler broadened width of the C VI line.

In addition to the measurements of the ion temperature via spectroscopy, TRANSP also provides an ion temperature estimate, assuming neoclassical confinement of the ions. The TRANSP predictions of ion temperature agreed well with the measurements; the comparison is shown in Figure 11 (a-d). The impurity ion temperature measurements extend over a modest time window, and are only available in the hot core plasma. Except possibly for the radial profile comparison at $t=0.472$ seconds, the agreement between the TRANSP calculation and the data is excellent.

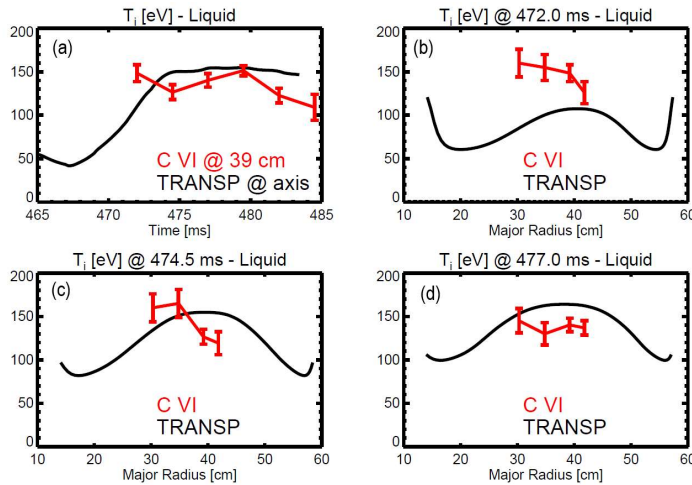


Figure 11. (a) Core ion temperature vs. the TRANSP neoclassical calculation, within 1-2 cm of the plasma axis, and (b-d) Comparison of the available radial profiles of the ion temperature data for three times within the discharge.

Reconstructions and energy confinement

TRANSP analysis has been performed for the hot and cold wall discharges, for which Thomson scattering is available. The TRANSP analysis assumed neoclassical ion confinement, which previously (for the 2020 Notable report) resulted in ion temperatures which matched the measurements from CHERS, although again CHERS was not available for the 2021 discharges. Figure 12 shows kinetic TRANSP results for the plasma current, ohmic power input, stored energy, electron energy confinement time, and total confinement time for both hot and cold walls.

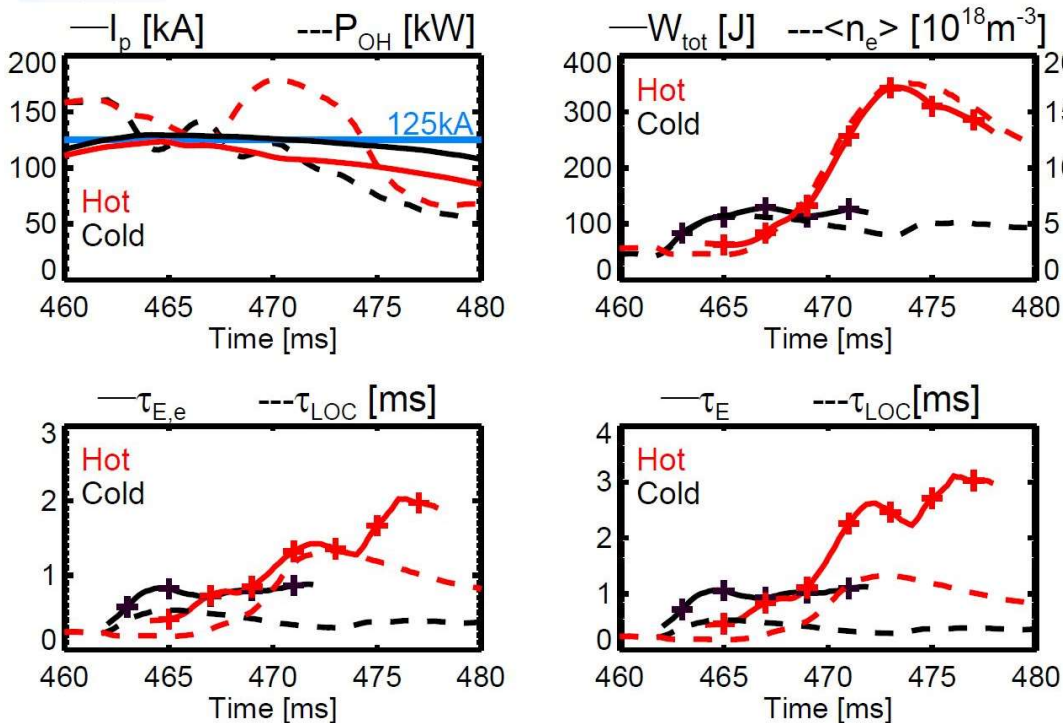


Figure 12. Input power, stored energy, and confinement from TRANSP kinetic calculations.

A comparison with Alcator Linear Ohmic Confinement (LOC) scaling is also shown. The TRANSP modeling uses an ensemble of discharges for both the cold and hot shell cases, since the LTX- β Thomson scattering system only produces one radial profile per discharge. Multiple discharges are required to document the temporal evolution of the discharge. For this data, multiple discharges at each time point were also taken to reduce the scatter in the Thomson scattering data.

Currently the Psi-Tri (C. Hansen, U. Washington) code is used to generate equilibrium reconstructions for LTX- β discharges. In Figure 13 we show equilibrium reconstructions for a cold shell discharge (a), and a hot shell discharge (b).

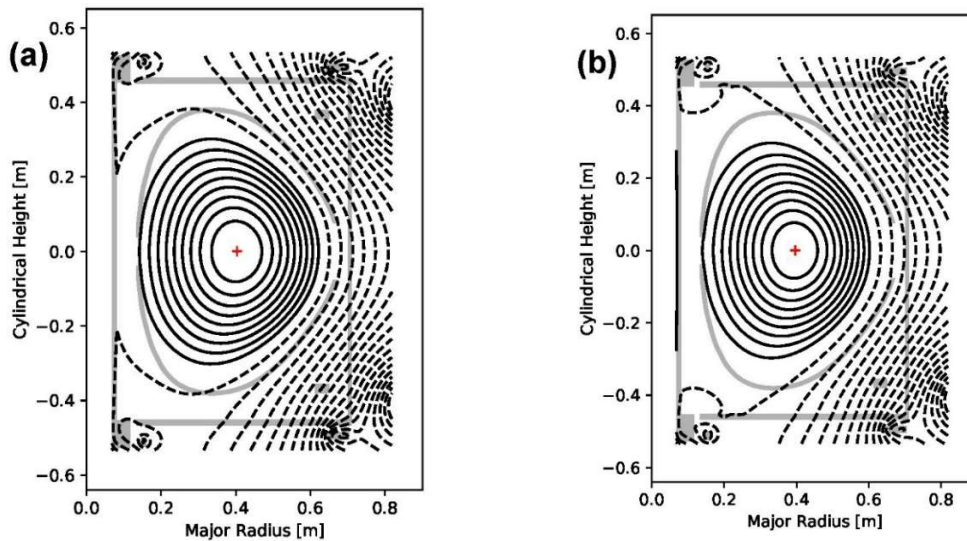


Figure 13. Equilibrium reconstructions from the U. Washington Psi-Tri code, for (a), discharge 102989, during cold shell operations, and discharge 103216, during hot shell operations. Based on the reconstructions, both discharges were high field side limited.

The Psi-Tri code also provides estimates of the stored energy and confinement time, using either magnetically or kinetically constrained reconstructions. A comparison of the results, based both on kinetic and magnetic measurements, is shown in Figure 14. For the kinetic estimates, the electron temperature is taken from the Thomson scattering data, and the ion temperature at the core is taken from the spectroscopic measurement for C VI in the core. The core ratio of T_i/T_e is approximately 0.75. In order to estimate the full stored ion energy, it is assumed here that this ratio is constant throughout the plasma radial profile. Note that this approximation produces good agreement between the kinetic estimate of confinement (“Kin”), and the magnetic estimate (“Std”). The Psi-Tri estimate of energy confinement exceeds the TRANSP estimate by an approximate factor of 2.

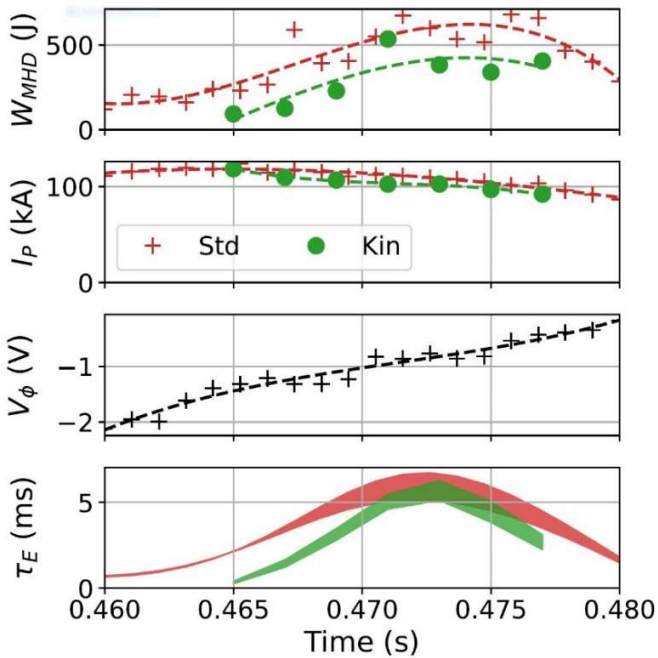


Figure 14. Magnetic and kinetic estimates for the confinement time from the Psi-Tri code, for the hot shell discharge (103216) equilibrium shown in Figure 13(b). Here the ion temperature is assumed to be $0.75 \times T_e$, consistent with the available ion temperatures from C VI broadening. The confinement times from Psi-Tri are higher than TRANSP modeling indicates for the hot shells.

Discussion of confinement

It would be informative to have discharges with fully passivated walls to compare with discharges run against fresh lithium plasma facing surfaces. Although we have recently been able to operate with fully passivated lithium walls, the resulting discharges ran at low current, and we did not obtain Thomson scattering data of sufficient quality for TRANSP analysis. We have SOL plasma comparisons with fully passivated walls (see Figure 6), but no confinement analysis. LTX-β is currently undergoing maintenance, and we expect to operate the tokamak in mid-July before applying a fresh coat of lithium, in order to obtain baseline (high recycling) discharges for comparison.

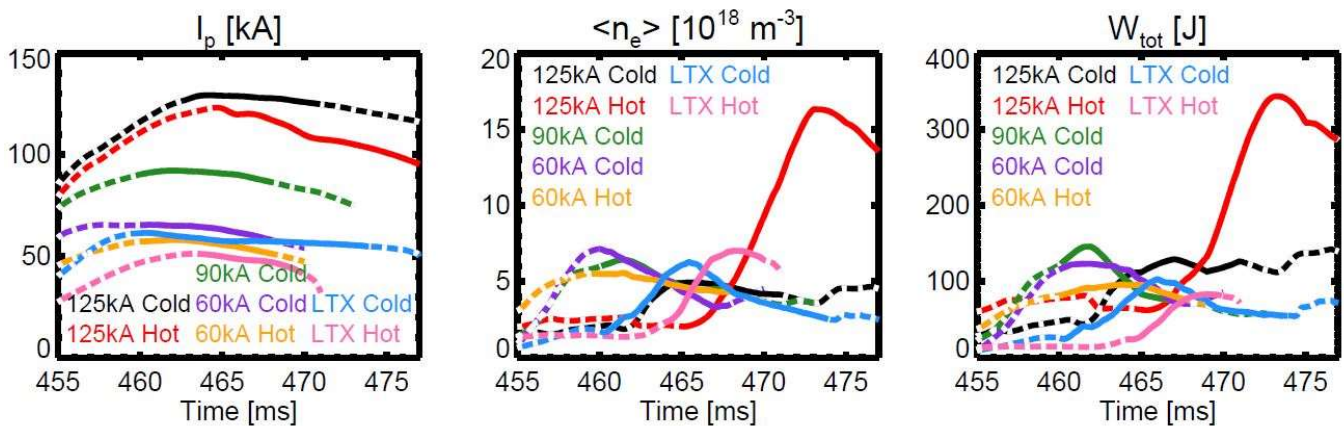


Figure 15. Plasma current, average density, and stored energy for LTX and LTX-β discharges for which reliable kinetic measurements are available. The dashed lines indicate data which is outside the window for which Thomson scattering profiles are available.

In Figure 15 we show comparisons of plasma current, density, and stored energy for the original 2015 LTX flat T_e discharges (LTX Cold), LTX data from late 2014 (LTX Hot), hot and cold shell data from

LTX- β in 2020 prior to the ohmic power supply upgrade; and the 2021 data. Before the upgrade to the ohmic power supply was completed earlier this year, plasma currents were limited to ≤ 90 kA for repeatable discharges, which could be assembled into a data set suitable for analysis with TRANSP. Most of the available data was for discharges in the 60 – 70 kA range. Hence the discharges from LTX in 2020 operated at plasma currents comparable to the LTX- β discharges in 2014 and 2015. Since 2016, we have focused on TRANSP modeling of LTX and LTX- β discharges. TRANSP provides very complete modeling of ohmic heating in time-dependent discharges, and discharges in LTX- β are too short to approach a steady-state.

Also, during the 2020 campaign, we were unable to obtain hot wall discharges with plasma currents comparable to the highest current discharges with cold walls. For the most recent campaign, we found that improved programming of the breakdown and current ramp, along with a modest increase in fueling at the very beginning of the discharge, enabled higher current operation with hot walls. During hot wall operation we also employed a large gas puff near the peak in the plasma current, which resulted in a large increase in density, and an attendant increase in stored energy. This large gas puff was advantageous for hot wall operation at high current in order to avoid flat-top MHD that otherwise degraded plasma reproducibility and would have made TRANSP analysis difficult. A comparable set of high-density discharges with cold walls will be performed when operations resume.

In Figure 16 we show the energy confinement time, confinement enhancement factor over Linear Ohmic Confinement (LOC) scaling, and the confinement factor over ITER H98 scaling. Note that the

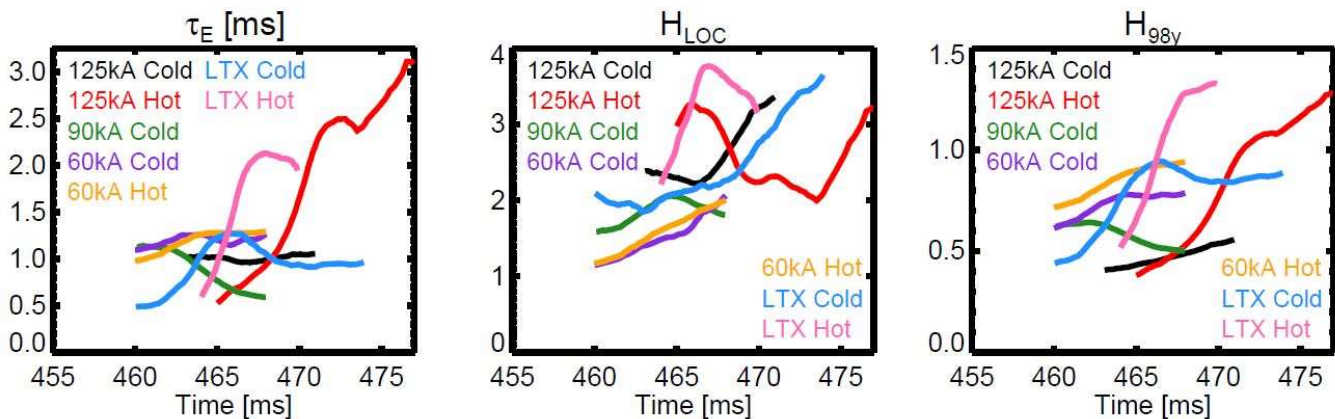


Figure 16. Energy confinement, enhancement factor over Alcator scaling, and enhancement factor over ITER 98 H-mode scaling.

LTX- β plasma is limited on the high field side, not diverted, and does not exhibit characteristics of H-mode discharges, so that the relevant confinement scaling is probably LOC. The highest absolute confinement times were produced in the hot wall discharges in 2021. The hot wall discharges also had the highest confinement enhancement factor over H98y scaling. Interestingly, the data indicates that confinement, or confinement enhancement (for the 2015 data), was increasing as a function of time for many of the discharges. Clearly, longer discharges with more control over the current ramp-up phase should be a future focus.

MHD activity

These discharges were not quiescent, but showed significant MHD activity. The LLNL group responsible for many of the edge plasma diagnostics on LTX- β maintains edge filterscope and fast camera diagnostics. In Figure 17 we show the behavior of the integrated line density, Li I line intensity, and hydrogen Lyman- α signal, along with the plasma current, for the cold shell discharge reconstructed in Figure 11(a), 102989. Density oscillations can clearly be seen in the line-integrated density from the interferometer, and are correlated with oscillations in both the Li I emission and the Lyman- α signal. MHD activity is visible in both the cold and hot shell cases, and may be responsible for enhanced transport in these discharges. At 0.485 seconds a particularly large crash, which results in a plasma current excursion, is seen.

Evidence of MHD activity can also be found in the fast camera images. Figure 18 (a&b) shows fast camera images of the outer shells in LTX- β just prior to, and during, the 0.485 second mode crash.

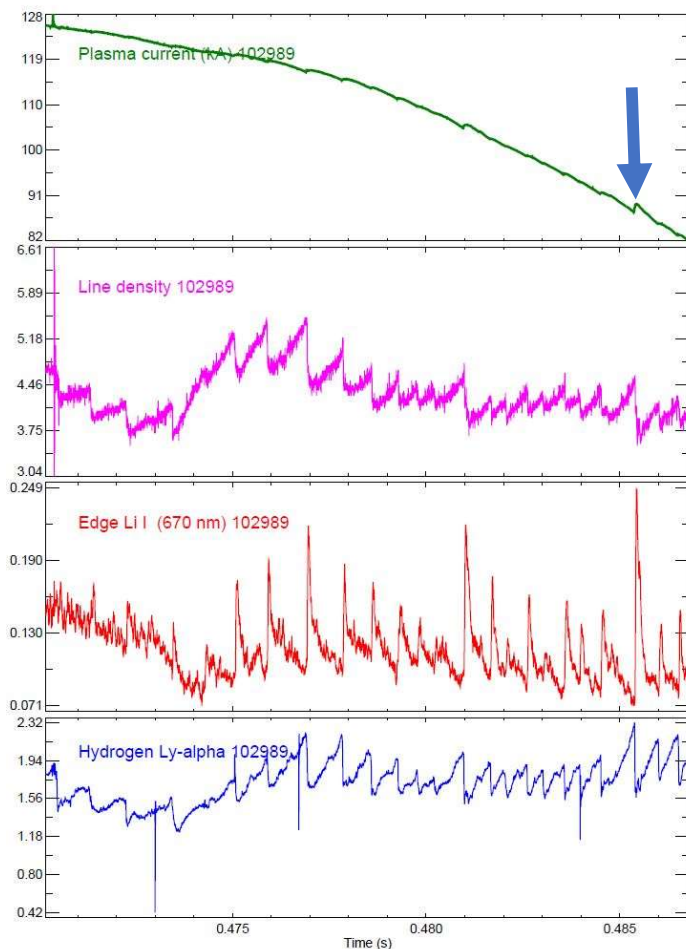


Figure 17. Evidence of MHD activity can be seen in the line density and edge filterscope data.

Numerous minor and major internal reconnection events (IREs) can also be seen in the plasma current traces for 2021 shown in Figure 4. The current ramp rate in these discharges is 10 MA/sec. over an appreciable part of the current buildup. Since these low recycling discharges have significantly higher electron temperatures than high recycling discharges, near the last closed flux surface, a 10 MA/sec. current ramp rate may not allow sufficient time for current to diffuse in, possibly leading to double

tearing modes and other MHD activity. As a part of future discharge development, we will investigate lower current ramp rates, and look for MHD quiescent operating regimes.

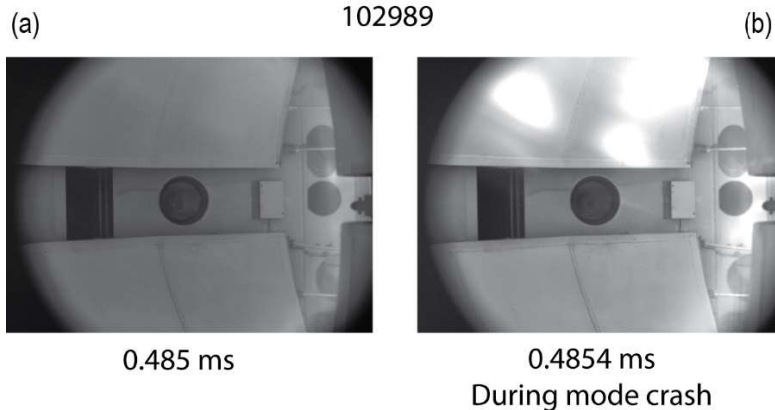


Figure 18. Images from the fast camera, viewing the outer shell surfaces and vacuum vessel, (a) just prior to the mode crash, and (b) at the mode crash, for discharge 102989.

Reasons for the delay in achieving this milestone

Research on LTX- β was interrupted by a pair of arcs involving the TF coil set, which at this point is well over 40 years old. The second of these arcs occurred in the final weeks before the original due date of the milestone. Repairs were originally estimated to take five weeks, but required a little over six weeks, including testing of the repaired coil set. Subsequent to the completion of the final TF repairs a number of facilities issues, including a failure of the pump delivering deionized water to the LTX- β power supplies, resulted in a further two week outage. Finally, two short sitewide outages of potable water forced evacuation of the laboratory, and delayed the final completion of the milestone tasks until the third week of June.

Earlier in FY21, a significant cause for the delay in LTX- β progress was the global pandemic. The LTX- β program lost six traceable weeks to COVID outages and quarantines. We also estimate that $\sim 20\%$ extra time was required for tasks performed from October 2020 through the end of March 2021, due to COVID protocols, occupancy limits for the LTX- β test cell, changes in procedures, etc. This amounts to an additional 4 week delay, due to the pandemic.

In addition, approximately 7 weeks of runtime (most, but not all of which, was additive to the 10 weeks noted above) was lost due to unscheduled facilities outages in chilled water and AC power.

SUMMARY

An upgrade to the ohmic power supply for LTX- β has resulted in an increase in the maximum plasma current to >135 kA. This new capability enabled achievement of record electron temperatures for both solid and liquid lithium walls, of 300 – 400 eV. Flat electron temperature profiles have also been recovered, for the first time since 2015 operation of LTX. TRANSP confinement analysis was also performed for cold and hot wall operation at high current and elevated confinement times were achieved with hot walls at high plasma density. Additional shot development is needed to be able to compare confinement times at elevated current with different wall conditions (passivated, cold Li, hot Li) and similar plasma densities and with and without beam heating. Additional capabilities, including new, higher capacity lithium evaporators, and a supersonic gas injector, have been implemented as well. The research program has now achieved the operational goals set out in the first FY21 Notable. This achievement was not accomplished by the milestone due date (end of March, 2021) due to delays

imposed by the global pandemic, two TF coil arcing events, and a number of facility infrastructure failures.